JOURNAL OF AERONAUTICAL

SCIENCE AND ENGINEERING

VOLUME.1

FEBRUARY 28, 2015

ISSN: 2442-6407

PUBLISHED BY ISOMAse

Journal of Aeronautical
-Science and Engineering-
Vol.1: February, 28 2015

Contents

ISOMAse

International Society of Ocean, Mechanical and Aerospace
-Scientists and Engineers-

Journal of Aeronautical
-Science and Engineering-
Vol.1: February 28, 2015

About JAse

The **Journal of Aeronautical -science and engineering- (JAse),** ISSN's registration no: 2442-6407 is an online professional journal which is published by the International Society of Ocean, Mechanical and Aerospace -scientists and engineers- (ISOMAse), Insya Allah, four volumes in a year which are February, May, August and November.

The mission of the JAse is to foster free and extremely rapid scientific communication across the world wide community. The JAse is an original and peer review article that advance the understanding of both science and engineering and its application to the solution of challenges and complex problems in subsea science, engineering and technology.

The JAse is particularly concerned with the demonstration of applied science and innovative engineering solutions to solve specific aeronautic industrial problems. Original contributions providing insight into the use of computational fluid dynamic, heat transfer, thermodynamics, experimental and analytical, application of finite element, aircraft systems, air transportation, air traffic management, and multidisciplinary design optimization of aircraft, flight mechanics, flight and ground testing, flight safety, integration of propulsion and control systems, wing in ground effect, structural design and dynamics, aeroelasticity, and aeroacoustics from the core of the journal contents are encouraged.

Articles preferably should focus on the following aspects: new methods or theory or philosophy innovative practices, critical survey or analysis of a subject or topic, new or latest research findings and critical review or evaluation of new discoveries.

The authors are required to confirm that their paper has not been submitted to any other journal in English or any other language.

ISOMAse

International Society of Ocean, Mechanical and Aerospace
-Scientists and Engineers-

Journal of Aeronautical
-Science and Engineering-
Vol.1: February 28, 2015

Scope of JAse

JAse welcomes manuscript submissions from academicians, scholars, and practitioners for possible publication from all over the world that meets the general criteria of significance and educational excellence. The scope of the journal is as follows:

- Application of Computational fluid dynamic in aeronautic
- Heat transfer and thermodynamics
- Experimental and analytical of Aircraft
- Application of finite element on structural design and dynamics
- Aircraft systems, air transportation, air traffic management
- Multidisciplinary design optimization of aircraft
- Flight mechanics, flight and ground testing, flight safety
- Integration of propulsion and control systems
- Aeroelasticity and aeroacoustics
- General aviation, military and civilian aircraft, WIG, UAV, STOL and V/STOL, subsonic, supersonic, transonic, and hypersonic aircraft.

The International Society of Ocean, Mechanical and Aerospace –science and engineering is inviting you to submit your manuscript(s) to isomase.org@gmail.com for publication. Our objective is to inform the authors of the decision on their manuscript(s) within 2 weeks of submission. Following acceptance, a paper will normally be published in the next online issue.

ISOMAse

International Society of Ocean, Mechanical and Aerospace
-Scientists and Engineers-

Journal of Aeronautical
-Science and Engineering-
Vol.1: February 28, 2015

Editors

Published

ISOMAse,
Jalan Sisingamangaraja
d/a Resty Menara Hotel
No.89 Pekanbaru-Riau
Indonesia
http://www.isomase.org/

Edited

P-23, Department of
Aeronautics, Automotive &
Ocean Engineering,
Faculty of Mechanical
Universiti Teknologi Malaysia
http://web1.fkm.utm.my/

ISOMAse

International Society of Ocean, Mechanical and Aerospace
-Scientists and Engineers-

Journal of Aeronautical
-Science and Engineering-, Vol.1

February 28, 2015

Wind Tunnel Test on Generic Agusta-Bell 206B Helicopter Tail Rotor Blades

Firdaus[a], Jaswar Koto[a,b,*], I.S. Ishak [a] and M.S. Ammoo[a]

[a)]*Department of Aeronautical, Automotive and Ocean Engineering, Faculty of Mechanical Engineering, Universiti Teknologi Malaysia*
[b)]*Ocean and Aerospace Research Institute, Indonesia*

*Corresponding author: jaswar@mail.fkm.utm.my and jaswar.koto@gmail.com

Paper History

Received: 16-February-2015
Received in revised form: 22-February-2015
Accepted: 27-February-2015

ABSTRACT

A low speed wind tunnel test was conducted for a full-scaled generic model of Agusta-Bell 206B helicopter tail rotor blades in the Universiti Teknologi Malaysia-Low Speed Tunnel (UTM-LST). The purpose of this paper is to conduct the experimental research for gaining information on general aerodynamics and performance characteristics of tail rotor blades. The lift and drag coefficients are examined in order to explore aerodynamic characteristics of the tail rotor blades. The present results may be useful to understand general aerodynamic characteristics and will be used in validation of the Quasi-Continuous Method (QCM) in the future.

KEY WORDS: *Wind Tunnel Test; Helicopter Tail Rotor Blades; Quasi Continuous Method.*

NOMENCLATURE

VLM	Vortex Lattice Method
MFM	Mode Function Method
QCM	Quasi Continuous Method
SSPM	Simple Surface Panel Method
CFD	Computational Fluid Dynamic
RPM	Revolutions per Minute

1.0 INTRODUCTION

The propeller blade is the device that mainly used as propulsive for marine vehicles, airplanes and rotorcraft. As it is a crucial part, it has to be designed to meet power requirement at the indicated speed with optimum efficiency. Now days, with growing demands for of higher speed and greater power, the propeller is becoming increasingly larger in size and its geometry shape become more complicated. Due this complicated geometry, the propeller should be optimally designed for increased propulsion efficiency.

To predict the steady and unsteady propeller characteristics, many numerical models and propeller theories were proposed. One of them and will be used in this study is based on lifting surface theory. The lifting surface theory also plays as important role in the hydrodynamic analysis of marine propellers. The theory has been developed for a long time in the field of aeronautics. While almost all of the applications of the theory are to wings of airplanes, there is an old application to screw propellers (Kondo, 1942).

A number of methods based on lifting surface theory to estimate the propeller characteristics have been published. They can be classified into two groups. One group is based on the continuous loading method such as Mode Function Method (MFM) and the other the discrete loading method such as Vortex

Lattice Method (VLM). Due to the complexity in numerical calculation using MFM, its application to unconventional propellers is not easy. VLM, however, also has some room to be improved; in the neighborhood of leading edge, the vortex strength predicted by VLM is always lower compared with analytical solutions. Owing to the discrete and concentrated loading distribution, pressure distribution is not estimated straightforwardly. Leading edge suction force is not estimated straightforwardly either. A large number of elements are necessary to get converged solutions (Naoto Nakamura, 1985).

Taking the above circumstances into consideration, a numerical method to estimate aerodynamics characteristics of helicopter tail propeller based on Quasi-Continuous Method (QCM) will be developed. QCM has both advantages of continuous loading method and discrete loading method; loading distribution is assumed to be continuous in chord-wise direction and stepwise constant in span-wise direction. Simplicity and flexibility of the discrete loading method are also retained.

To validate this method, experimental procedure has been proposed with used the full scaled generic model tail rotor blades of Agusta- Bell 206B helicopter that was conducted in the UniversitiTeknologi Malaysia- Low Speed Tunnel (UTM-LST). Present data show the aerodynamic characteristics, lift coefficient and drag coefficient of the blade. And the sample data in time series at the angle of attack and speed selected will also present.

2.0 EXPERIMENTAL ARRANGEMENT

2.1 Wind Tunnel

The test was conducted in the UniversitiTeknologi Malaysia-Low Speed Tunnel (UTM-LST). The layout of wind tunnel aerodynamic circuit and indicates the important components within the wind tunnel circuit are illustrated in Figure 1.

The UTM-LST is a pressurized, closed-circuit, continuous-flow wind tunnel with an operating pressure from approximately 0.10 to 4 atmospheres. The test section size is 2.0 m wide x 1.5 m height x 5.5 m length. The wind tunnel has an excellent flow quality (flow uniformity < 0.15%, temperature uniformity < 0.2%, flow angularity uniformity < 0.15%, turbulence < 0.06%) that was mentioned in the AIAA paper (Elfstrom GM, 2007). And it is capable of delivering maximum airspeed of 80 m/s (160 knots or 288 km/hr) inside the test section (Alias Mohd Noor, 2013).

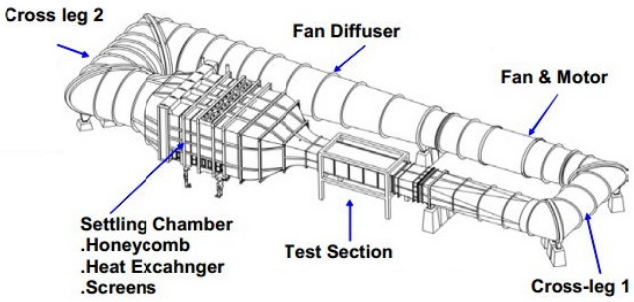

Figure 1: Wind tunnel components.

2.2 Tail Rotor Blade Model

Figure 2 shows the blades from the generic model of the tail rotor blades from Agusta-Bell 206B helicopter, with an actual scale will be used in this experiment. The blade was 720mm overall length and has 134mm length of the chord.

The airfoil profile of the blade is near similar to NACA 0012 series, with maximum thickness 12% at 33% chord as shown in Figure 3.

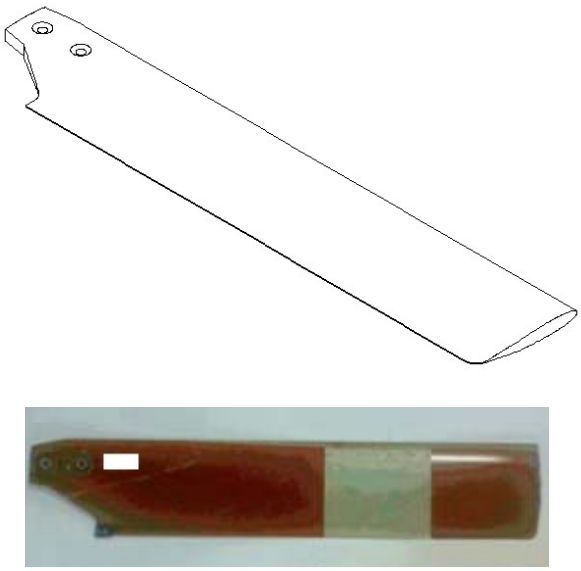

Figure 2: Used Bell B206 tail rotor blade

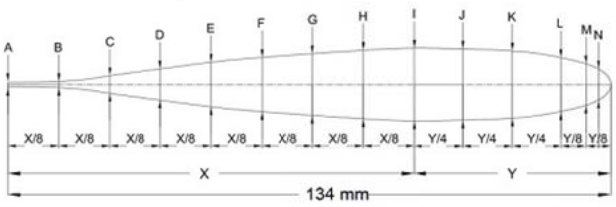

Figure 3: Airfoil profile of tail rotor blade.

2.3 Tests and Methods

To measure the aerodynamic characteristics, lift, drag and pitching-moment, the tail rotor blade was supported by a bracket that attach to force balance sensor. Figure 4 shows the schematic diagram of the tail rotor blade configuration in this experiment that mounted on force balance sensor via bracket support.

The type force balance sensor that's been used in this experiment is portable JR3 Force Balance, Figure 5. The balance has a capability to measure the aerodynamic forces and moment in 3-dimensional. The aerodynamic loads can be tested at various wind direction by rotating the model via the turntable. The accuracy of the balance is within 0.04% based on 1 standard deviation.

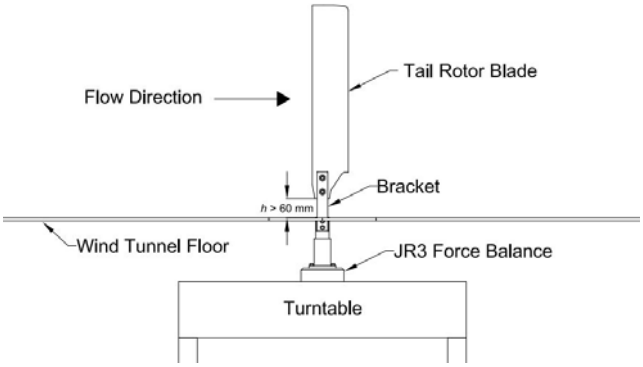

Figure 4: Schematic diagram of model-balance arrangement.

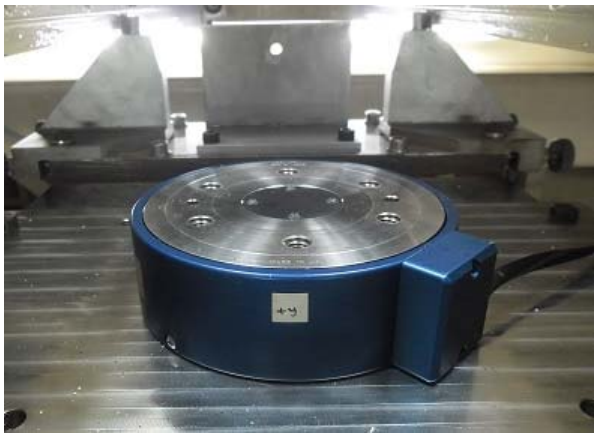

Figure 5: JR3 external force balance.

In this experiment, the wind tunnel speed was set from 5 m/s to 40 m/s, corresponds to a Reynolds number based on airfoil chord from 0.419×10^5 to $3.352 \times 10^5$and angle of attack of 0, 5, 10, 12, 15, 18, 20, and 25 degrees. Since the blockage ratio is merely small, blockage corrections are assumed to be negligible.

Table 1 shows the set up air speed data from the wind tunnel.

Table 1: Wind tunnel air speed data

Speed, V	Reynolds Number (Re) × 10^{-5}	RPM	Pressure, mbar
5	0.419	54.0	14.7
10	0.838	103.5	59.1
15	1.257	152.5	133.2
20	1.676	200.5	235.5
25	2.095	249.0	368.8
30	2.514	297.0	530.8
35	2.933	345.0	721.8
40	3.352	393.0	945.4

In order minimize the sidewall boundary-layer interference effects on the balance measurements, the blade model was placed distance from the floor. The gap of 60 mm was provided between lowest parts blade model and upper surface wind tunnel floor to minimize airflow and provide clearance for balance measurement, Figure 4 and Figure 5 shown the gap in the between of the blade bracket that has been mounted with a force balance sensor which position under the wind tunnel floor.

The laminar-separation and turbulence-reattachment location were determined using the oil dot technique. The smoke test follows up after the oil dotted test already done. The objective this test is to visualize the flow pattern on the blade, before and after the stall angle happen to the blade. The typical result for this test is shown Figure 9.

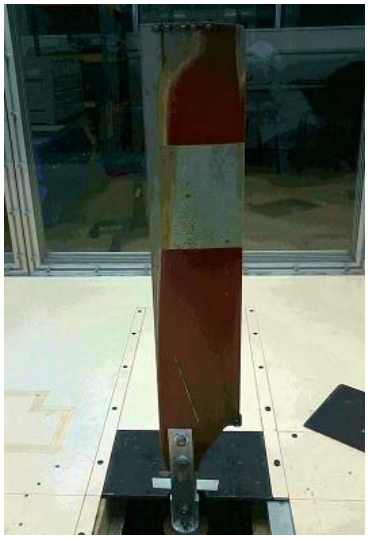

Figure 6: Gap between tail rotor blades with wind tunnel floor.

3.0 AXIAL, NORMAL, LIFT, AND DRAG FORCE DIRECTIONS PROCEDURE

The force coefficient F_X and F_Y are parallel and perpendicular to the chord line of the blade, whereas the more usual coefficient F_L

and F_D are defined with reference to the direction of the free-stream airflow. (E.L Houghton, 2013)

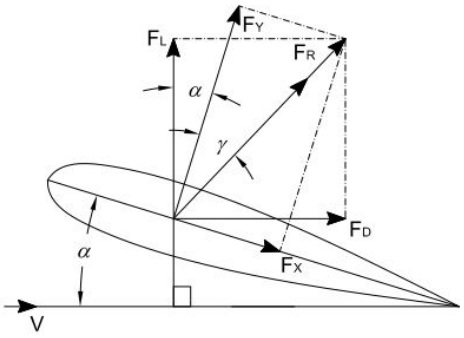

Figure 7: Definition: axial, normal, lift, and drag force directions.

The conversion from one pair of coefficient to the other may be carried out with reference to Figure 7 which is F_R, the coefficient of the resultant aerodynamic force, act at an angle γ to F_Y. F_R is the result both of F_X and F_Y and of F_L and F_D: therefore, based on the Figure 7, it can defined that

$$F_L = F_R\cos(\gamma + \alpha) = F_R\cos\gamma\cos\alpha - F_R\sin\gamma\sin\alpha \quad (1)$$

But $F_R\cos\gamma = F_Y$ and $F_R\sin\gamma = F_X$, so

The lift force is defined by:

$$F_L = F_Y\cos\alpha - F_X\sin\alpha \quad (2)$$

Similarly, the drag force also defined by:

$$F_D = F_R\sin(\gamma + \alpha) = F_Y\sin\alpha + F_X\cos\alpha \quad (3)$$

And finally, the coefficients are given by the relationships

$$\text{Lift coefficient, } C_L = \frac{F_L}{\frac{1}{2}\rho V^2 S} \quad (4)$$

$$\text{Drag coefficient, } C_D = \frac{F_D}{\frac{1}{2}\rho V^2 S} \quad (5)$$

4.0 RESULT AND DISCUSSION

The aerodynamic characteristics of the tail rotor blade were measured by using external balance system. As mentioned previously, the test wind speed was set from 5 m/s to 40m/s with increment 5 m/s for every test, and the blade setting angle of attack for this test is 0, 5, 10, 12, 15, 18, 20, and 25 degrees.

To correctly subtract the interface drag, the additional test with only bracket without tail rotor blades with similar condition such as air speed and angle of attack was executed.

Before starting the test, a tare reading was taken for every test with the wind off (where air speed is equal to 0 m/s) to get a measurement of the bias data.

Repeatability tests had also be conducted to ensure getting precise reading and validate the quality of measured results. Figure 8 depicts the sample reading in a time series data for angle of attack 15 degrees and air speed set to 40 m/s from the external balance sensor.

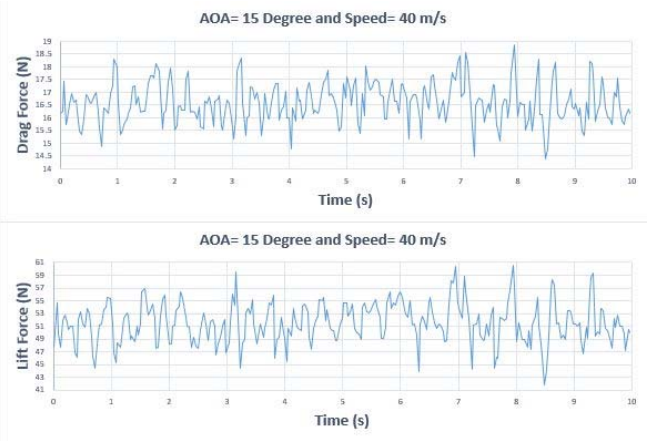

Figure 8: Time series data from external balance sensor.

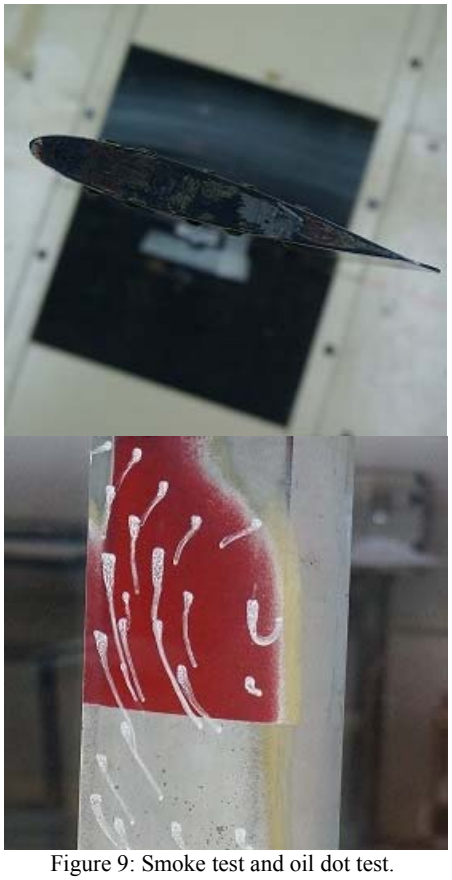

Figure 9: Smoke test and oil dot test.

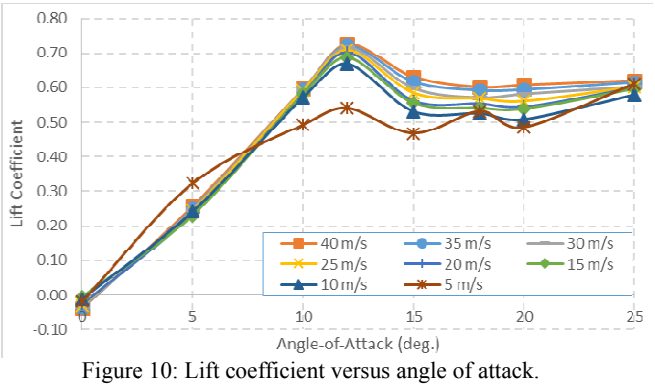

Figure 10: Lift coefficient versus angle of attack.

Graph in figure 10 shows the lift coefficient variations with different air test speed. At an angle of attack 12-13 degree shows the peak of lift coefficient where maximum lift happens before it drops after this points. And this condition is a critical or stalling angle of attack where the tail rotor blade starts to be less efficient to generate lift after beyond this angle of attack.

The reason the stall happens in the first place is because the air under heavier pressure beneath the blade finds it easier to creep forwards over the upper surface from the trailing edge as the angle against the relative airflow increases, because the upper air has started to slow down and now has an unfavorable pressure gradient, past the suction peak. It has longer to travel and more surface friction to cope with, so it doesn't have the energy to keep flowing and create the same pressure differential, and the amount of lift is reduced (the pressure at the trailing edge is atmospheric anyway). As the boundary layer has less momentum, it works harder keeping to surface (Phil Croucher, 2013).

Boundary layer separation is therefore produced from the adverse pressure gradient, when air start flowing in the reverse direction of the free stream, forcing itself under the normal airflow which has started to slow down. This flow we can see through the smoke and oil dot test like in Figure 9. This test will shows the patterns of airflow on the blade, before and after stalling angle happen.

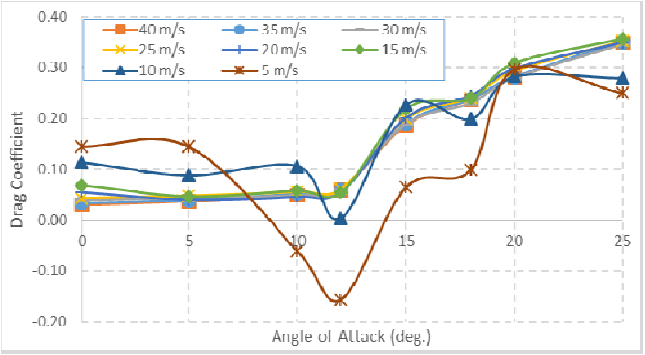

Figure 11: Drag coefficient versus angle of attack.

Although the lift force is still can be produced after that angle, the blade has a hard time to generate it. Stalling can alleviate by increasing the speed of airflow on the blade. But this will be lead to an increment of drag coefficient of tail rotor blades as shown in Figure 11. After the angle of attack 12-13 degrees, the drag coefficient rapidly increased, corresponds to an increment of angle of attack and speed of airflow. The coefficient of drag becomes steady after airflow speed achieved 15 m/s and above. However it is should be noted both Figure 10 and Figure 11 indicate bad readings for data taken at V=5 m/s. This is because at a very low speed as 5 m/s, the flow is slightly fluctuated since UTM-LST is not built for the low speed flow experiment.

6.0 CONCLUSION

The general aerodynamics and performance characteristics of the full scaled generic model tail rotor blades of Agusta Bell 206B helicopter by experimental works have been obtained at speed 5 m/s to 40 m/s, corresponds to a Reynolds number based on airfoil chord from 0.419×10^5 to 3.352×10^5 in the UniversitiTeknologi Malaysia-Low Speed Tunnel (UTM-LST). The tests were conducted in a manner as to minimize both experimental apparatus and instrumentation uncertainties. Nevertheless it is conceded that there could be discrepancies with the exact data of the 206B rotor tail blade since some assumptions had been made, and due to limitations of experimental set-up during the wind tunnel testing.

REFERENCE

1. Alias Mohd Noor and Shuhaimi Mansor. 2013. *Measuring Aerodynamic Characteristics Using High Performance Low Speed Wind Tunnel at Universiti Teknologi Malaysia.* Transport Research Alliance, Universiti Teknologi Malaysia.
2. E.L. Houghton, P.W. Carpenter, Steven Collicott and Dan Valentine. 2012. *Aerodynamics for Engineering Students (Sixth Edition)*. Butterworth-Heinemann. Page: 54-55.
3. Elfstrom GM. 2007.*History of Test Facility Design Expertise at Aiolos, Engineering Corporation*. AIAA 45th AIAA Aerospace Sciences Meeting and Exhibit, Reno, Nevada, USA.
4. Firdaus Mahamad, Jaswar Koto, M.S Ammoo and I.S.Ishak, 2014, Application of Quasi-Continuous Vortex Lattice Method to Determine Aerodynamic Characteristics of Helicopter Tail Rotor Propeller, *Proceeding of Ocean, Mechanical and Aerospace -Science and Engineering-, Vol.1, pp.44.52*, Pekanbaru, Indonesia.
5. Hao Rui, Jaswar Koto, 2014, *Prediction of Propeller Performance Using Quasi-Continuous Method*, Journal of Ocean, Mechanical and Aerospace -Science and Engineering-, Vol.10, pp.12-18.

6. Mohd. Shariff bin Ammoo, Ziad Bin Abdul Awal, Jaswar Koto, 2015, *Air Flow Characteristics and Behaviour of Main Rotor Blade of Remote Controlled Model Scale Helicopter*, Journal of Ocean, Mechanical and Aerospace -Science and Engineering-, Vol.16, pp.18-22.
7. Naoto Nakamura. 1985. *Estimation of Propeller Open-Water Characteristics Based on Quasi-Continuous Method*. Spring Meeting of The Society of Naval Architects of Japan. Japan.
8. Phil Croucher. 2013. *Private Helicopter Pilot Studies JaaBw.* Electrocution (January 7, 2015).

Journal of Aeronautical
-Science and Engineering-, Vol.1

February 28, 2015

Effects of Reynolds Number on Flow Separation above Generic Half Span Transport Aircraft Model

Rhubbindran,[a,*] and Shabudin bin Mat,[b]

[a)] *Department of Aeronautics, Automotive and Ocean Engineering, Universiti Teknologi Malaysia, Johor Bahru Malaysia*

*Corresponding author: rhubbindran.sunthrasakaran@gmail.com and shabudin@fkm.utm.my

Paper History

Received: 18-February-2015
Received in revised form: 22-February-2015
Accepted: 26-February-2015

ABSTRACT

The purpose of this study is to investigate the flow separation on UTM half model at 3 different Reynolds number which is 0.5 x 10^6, 1.0 x 10^6 and 1.5 x 10^6 which corresponds to speed, V = 20 m/s, 45 m/s and 65 m/s using pressure distribution method and flow visualization. The study was done to observe the flow separation for three different Reynolds number. The pressure distribution at 50% wing span was measured and plotted to observe the flow characteristic at angle of attack from 0 deg to 24 deg at three different Reynolds number. The pressure distribution on the wing was reduced to local lift coefficient and this data was compared to lift coefficient obtained from the balance data to study when the model reaches stall.

KEY WORDS: *UTM Half Model; Wind Tunnel Experiments; Flow Visualization; Flow Separation.*

1.0 INTRODUCTION

This experiment is conducted to visualize the phenomena of flow separation that occurs on a generic transport aircraft model. The model which is going to be tested is a 9% scaled semi-span model of a generic passenger aircraft or called UTM half model. From the fundamental of aerodynamics, a particular wing will provide lift until a certain angle of attack, beyond this angle of attack the wing is said to reach stall where the flow on the top surface of the wing is said to be separated. Many factors affect the flow separation on a wing, for example the thickness of the wing section will contribute to leading edge stall (thin airfoil) or trailing edge stall (thick airfoil) but this is not our main interest. Instead, the experiment is conducted to investigate the effect of Reynolds number on flow separation. The experiment will be conducted under 3 different setting of velocity corresponding to 0.5 x 10^6, 1.0 x 10^6 and 1.5 x 10^6 Reynolds number. The flow separation test will be carried out in UTM LST (Low Speed Tunnel) itself. The model of 0.983m wing-span will be mounted in the wind tunnel test section with cross section of 1.5m height by 2m width. In order to visualize the flow around the wing of the semi-span model, pressure around the local chord at 50% span will be measured

2.0 LITERATURE REVIEW

2.1 Boundary Layer

Prandtl states that in order for flow separation from the wall to take place, the following condition must be satisfy which is increasing in pressure or adverse pressure gradient. Going downstream, a small amount of momentum and energy along the body surface is lost as they are used up to overcome pressure and friction. The downstream velocity and momentum are small near the body surface due to presence of viscosity. At one point, the fluid particle will lose all the momentum and brought to a halt, further downstream will cause the fluid particle to leave the surface and there will be a presence of reversed flow [1].

2.2 Reynolds Number

Reynolds number is a dimensionless parameter which is a measure of the ratio of inertia forces to viscous forces in a flow. In flow separation, Reynolds number is a dominant factor in transition to turbulent flow and we define it as critical Reynolds number, Recr. It is difficult to predict the exact value of Recr for a given body under specified conditions. Recr is approximated 500,000 as a rule of thumb in practical application, if the value of

Reynolds number is above 500,000 then the flow is said to be turbulent and if the Reynolds number is less than 500,000 then the flow is said to be laminar [2].

2.3 Laminar Separation

If the path line of the fluid element smooth and regular then the flow is laminar. Consequent to the previous statement, the layers are very thin and the form drag is small too [3]. Even though the velocity is large enough to give significant viscous stress but it is yet moderate and the skin friction is small too. Laminar boundary layer is prone to transition in adverse pressure gradient so it is hard to predict whether transition or flow separation occurs first. During laminar separation, the flow separates, transition and the reattaches back and this phenomenon is called laminar separation bubble as shown in the figure. As the angle of attack is increased, the adverse pressure gradient will be more severe and the separation bubble will burst and cause airfoil to stall.

2.4 Turbulent Separation

In turbulent boundary layers, the flows are not steady and smooth but eddying. Since the flow is eddying and not smooth, the boundary layer will be thicker compared to the laminar flow which results in greater form drag [3]. Turbulent flow separation can't be analyst analytically as laminar flow separation so experimental results are used for its solution.

2.5 Flow Separation on Swept Wing

Swept wing usually produces less lift compared to a straight wing with similar area and chord at all speed. The main problem of a swept wing aircraft is stall occurs at the tip due to the span wise airflow which is aggravated by the leading edge vortexing. Leading edge vortexing occurs when the air from the bottom of the wing jumps to the top of the wing and moves to the wing tip [4]. The stream wise growth of the boundary layer tends to cause early stall near the tips. Consequently the boundary layer gets more and more tired and less capable of surviving the adverse gradients without separating [5]. The leading edge vortexing, span wise flow and tip stalling tendency increases as the angle of attack of the aircraft is increased.

3.0 MODEL EXPERIMENT

3.1 UTM Half Model Specification

Table 1 shows the specification of the UTM half model which is a semi span model of a transport aircraft that is going to be tested for flow separations. The data are obtained from the manufacturer's blueprint as in Figure 2. Figure 1 shows a photo of the UTM Half Model, as it can be seen, it is a semi span model.

Figure 1: UTM half model

Table 1: Dimensions of the UTM half model

Symbol	Meaning	Dimension
S	Wing Area	0.252 m^2
c	Mean Aerodynamic Chord	0.339 m
b/2	Half-Span	0.983 m
V_{wing}	Wing Volume	0.00072 m^3
$V_{fuselage}$	Fuselage Volume	0.058 m^3

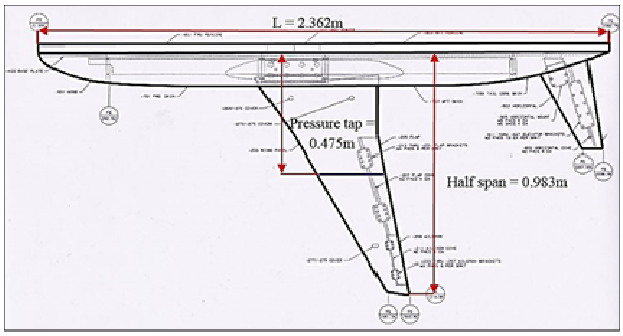

Figure 2: The dimension of the UTM half model

The pressure tabs are located 507mm from the wing tip or 50% wing span. The purple line in Figure 3.2 shows the pressure tap at 50% wing span. There are 18 ports of pressure tab where 9 ports on the upper surface of the wing and the remaining 9 port is located at the bottom surface of the wing. This pressure tabs will used to calculate the local pressure distribution. Table 2 shows the location of the pressure tap at 50% wing span.

Table 2: Location of pressure taps in x/c from the local leading edge.

No. of Pressure Taps	Suction Surface (x/c)	Pressure Surface (x/c)
1	0.0227	0.0227
2	0.0626	0.0626
3	0.1026	0.1026
4	0.1625	0.1625
5	0.2523	0.2523
6	0.3022	0.3022
7	0.4020	0.4020
8	0.6017	0.6017
9	0.9012	0.9012

3.2 Wind Tunnel Testing

The semi span model is installed in the UTM Low Speed Wind tunnel as in Figure 3. The angle of attack of the model is varied from angle of attack of 0 deg to 24 deg (which is the maximum angle of attack that the model can go when attached to the semi span balance). The test were conducted at 3 different velocities corresponding to its respective Reynolds number of 0.5 x 10^6, 1.0 x 10^6 and 1.5 x 10^6 to understand the effect of Reynolds number on flow separation.

The first flow visualization method that was used in conducting this experiment was by measuring the pressure distribution around the surface of the UTM Half model wing. Taking the data on the pressure distribution will give a clearer view where adverse gradient occurs on the wing.

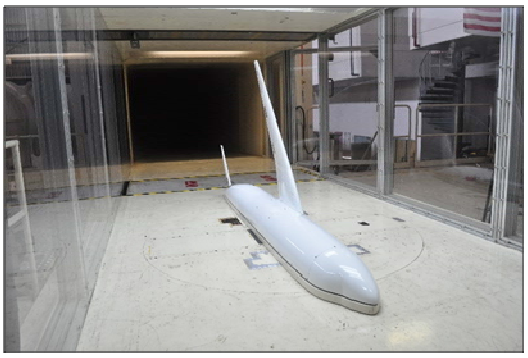

Figure 3: The installation of UTM half model attached to a semi span balance in UTM LST

Next flow visualization method that was used is tuft, where strips of yarn are attached on the surface of the UTM half model as in Figure 4. During the test, this tufts are recorded to study the flow features such as boundary layer separation and reattachments on the model. Tufting is a technique of flow visualization that is used in the aeronautics filed main to study air flow direction, strength and boundary layer properties

Figure 4: Threaded tuft used as a flow visualization method

3.3 Experimental Flow Chart

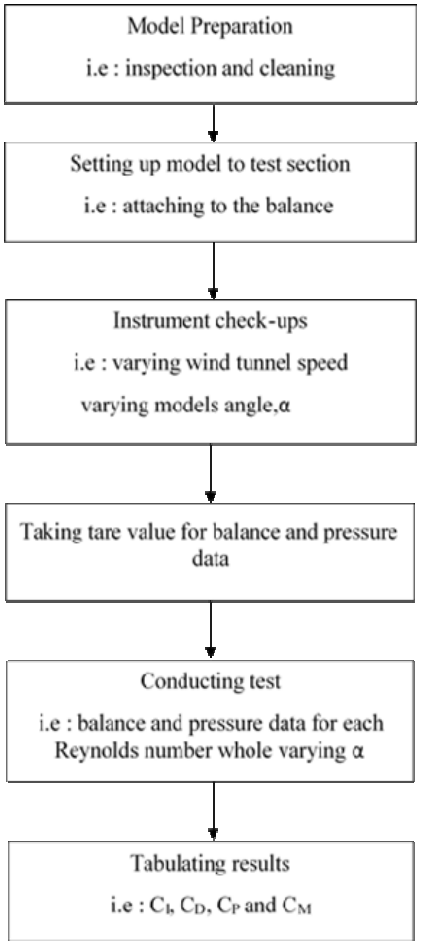

Figure 5: Experimental setup

4.0 ANALYSIS

4.1 Reynolds Number and speed approximation

The objective of this experiment is to test the UTM half model under three different Reynolds number which are 0.5 x10^6, 1.0 x 10^6, 1.5 x 10^6. The ratio of inertial forces or resistant to motion to viscous forces can be expressed by the Reynolds number. Reynolds number can be expressed in equation as below

$$\boldsymbol{Re} = \frac{\boldsymbol{V\,l}}{\boldsymbol{v}} \quad (1)$$

After deciding the Reynolds number, the wind speed that was tested in the wind tunnel can be found using the Reynolds number formula as shown below

$$\boldsymbol{V} = \frac{\boldsymbol{Re\,v}}{\boldsymbol{l}} \quad (2)$$

where V is velocity, l is mean aerodynamic chord of the model and ν is kinematic viscosity. The known value of the air density, mean aerodynamic chord and kinematic viscosity is constant and by adjusting the formula, certain value of the wind speed can be calculated for certain value of Reynolds number.

Table 3: Approximate wind speed for the wind tunnel experiments

Reynolds number	Wind Speed, V
0.5 x 10^6	20 m/s
1.0 x 10^6	45 m/s
1.5 x 10^6	65 m/s

4.2 Data Calculation

The obtained results are received from the Micro Craft MC-10.8.0-A semi span balance. The raw data have to be reduced to the wind axis in the following manner. Figure 4.1 shows the process from taking the raw data until converting it to the wind axis force coefficients:

$L = F_Z \cos\alpha + F_X \sin\alpha$

$D = F_X \cos\alpha - F_Z \sin\alpha$

$F_Y = 0$ (MC-10.8.0-A does not measure side force)

Coefficient of pressure is a parameter for studying incompressible flow and it is a dimensionless number which describes the relative pressures throughout a flow field in fluid dynamics. The formula for coefficient of pressure, C_p, is stated below:

$$\boldsymbol{C_P} = \frac{\mathbf{P}-\mathbf{P}_\infty}{\frac{1}{2}\boldsymbol{\rho}_\infty \boldsymbol{V}_\infty^2} \quad (3)$$

Where P is the pressure at the where pressure coefficient is calculated, $\mathbf{P}_\infty$ is the free stream pressure, $\boldsymbol{\rho}_\infty$ is the free stream air density and $\boldsymbol{V}_\infty$ is the free stream velocity of the fluid.

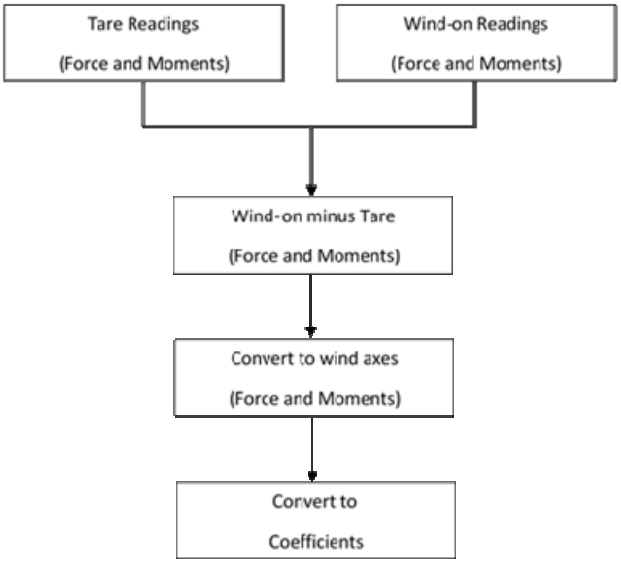

Figure 6: Flow chart for data reduction

5.0 RESULTS AND DISCUSSION

Figure 7 shows the measured pressure coefficient distribution around the UTM Half model at 50% wing span or the local chord, from an angle of attack of 0 deg to 24 deg at Reynolds number 0.5 x 10^6. The surface pressure distribution on the lower surface or the pressure surface of the wing notably does not change much after angle of attack 6 deg but the surface pressure distribution on the upper surface or the suction surface of the airfoil was found to significantly vary from angle of attack of 0 deg to 8 deg. From angle of attack of 10 deg to 24 deg, the surface pressure coefficient of the suction surface seems to be stagnant where it doesn't change much even though the angle of attack varies. As the angle of attack increases from 0 deg to 2 deg, it is notice that there is a region of nearly constant pressure at x/c ≈ 0.10 to 0.16 and from angle of 4 deg to 6 deg the constant pressure region moves forward to x/c ≈ 0.06 to 0.10. A sudden increase in surface pressure coefficient was found following the constant pressure region. Further downstream, the surface pressure coefficient gradually recovers back. This kind of characteristic of surface pressure profiles relates to laminar flow separation and the formation of laminar separation bubbles. As the angle of attack of the model is increased, the location of the separation point to the reattachment point is moving forward towards the leading edge of the wing.

Figure 8 and Figure 9 shows the coefficient of pressure for Reynolds number 1.0 x 10^6 and 1.5 x 10^6 respectively, both the flow shows that the pressure distribution on the pressure surface of the wing does not change much after angle of attack of 8 deg. Both the flows also show constant pressure distribution on the suction surface of the wing after angle of attack of 10 deg. Compared to the flow with Reynolds number 0.5 x 10^6, the flows with higher Reynolds experiences flow separation after angle of attack of 8 deg but the flow with Reynolds number 1.5 x 10^6

managed to sustain the flow at angle of attack of 10 deg with very high adverse pressure gradient. After 10 deg, the flow for the higher Reynolds number separates. The flows with higher Reynolds number which are 1.0 x 10^6 and 1.5 x 10^6 does not show signs of laminar separation as this flow is too high to be in the laminar regime. Both flows fully separates after an angle of attack of 8 deg which shows better sustainability compared to the flow with Reynolds number 0.5 x 10^6. All the 3 flows shows sign of leading edge separation where the flow detaches from the wing suction surface starting from the leading edge.

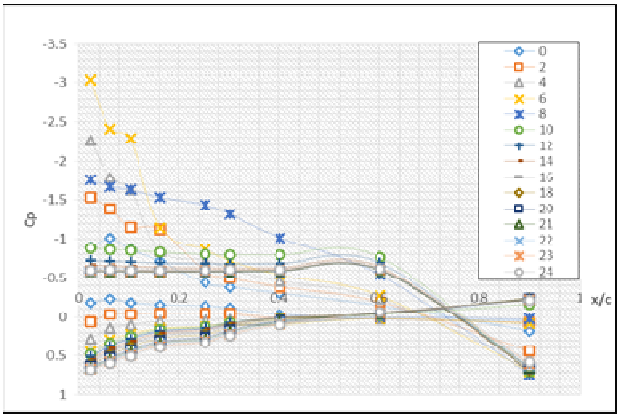

Figure 7: Surface pressure distribution profiles at 50% span at Re = 0.5x10^6 (V=20m/s)

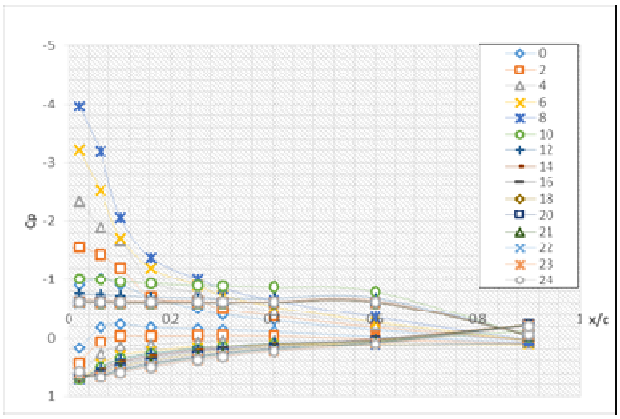

Figure 8: Surface pressure distribution profiles at 50% span at Re = 1.0x10^6 (V=45m/s)

From Figure 10, the coefficient of lift at the local chord is obtained from the area under the coefficient of pressure graph for three different Reynolds number. The method used to calculate the area under the graph is trapezoidal method so there will be some discrepancy in the result plotted in Figure 10 but it still shows at which angle of attack the local chord flow separates. At Reynolds number 0.5 x 10^6, the coefficient of lift rises rapidly until the maximum peak at the angle of attack of 8 deg and then decreases rapidly, so it is seen that the flow on the wing at the local chord fully separates after the angle of attack of 8 deg. The maximum peak of coefficient of lift at Reynolds number 1.0 x 10^6 falls in between angle of attack of 8 deg and 10 deg which is about at 9 deg. The result shows that by increasing the Reynolds number of the flow, the flow is delayed from separating at $\alpha = 8$ [Re = 1.5 x 10^6] to $\alpha = 9$ [Re = 1.0 x 10^6] and $\alpha = 10$ [Re = 1.5 x 10^6].

Figure 9: Surface pressure distribution profiles at 50% span at Re = 1.5x10^6 (V=65m/s)

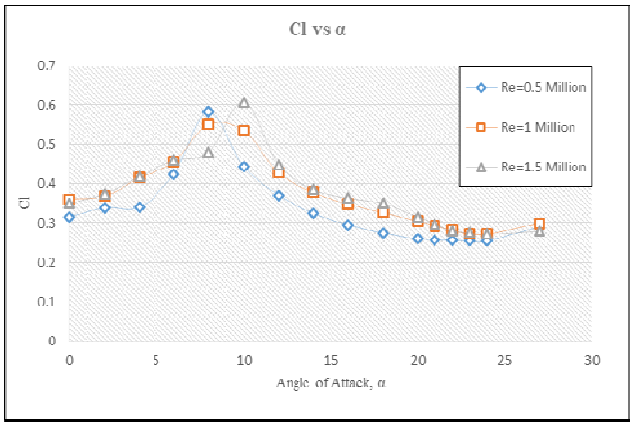

Figure 10: Coefficient of lift calculated from the area under the coefficient of pressure graph for 3 different Reynolds number

Figure 11 shows lift obtained from the balance and it can be seen that the UTM half model stalls after angle of attack of 8 deg for Reynolds number 1.0 x 10^6 and 1.5 x 10^6 which is nearly the same angle where the wing section at 50% span of the model produces the highest lift. This is almost the same for the flow with Reynolds number 0.5 x 10^6 where the model manage to have proportional lift curve slope until the angle of attack of 6 and hit the peak at 8 deg before going to a plateau stage and the wing section at 50% span also have almost the same characteristic as it separates beyond 8 deg angle of attack.

To further concrete the previous statements, Figure 12 and Figure 13 shows the flow visualization done using the threaded tuft for Reynolds number 1.5 x 10^6. The red line in both figures are drawn to indicate the location of the pressure taps at 50% span while the yellow lines indicates the region where the flow is separated. When both figures are compared, we can see that the

flow separation for a tapered-swept wing grows from the wing tip to the wing root. As stated previously that flow separation occurs after angle of attack of 10 deg for the flow with Re = 1.5 x 10^6 is proven in Figure 5.7. It shows that almost 70% area of the wing is experiencing flow separation, as this will dramatically cause the model to lose a lot of lift and this can be seen in Figure 5.5 where the balance data shows us that after angle of attack of 8 deg, the UTM half model reached stall.

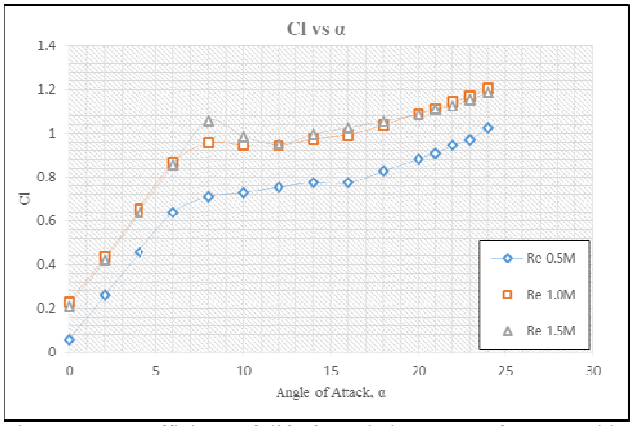

Figure 11: Coefficient of lift from balance test for Reynolds number 0.5 x 10^6, 1.0 x 10^6 and 1.5 x 10^6

Figure 12: Flow visualization using threaded tufts at α = 10° at Re = 1.5 x 10^6

Figure 13: Flow visualization using threaded tufts at α = 11° at Re = 1.5 x 10^6

6.0 CONCLUSION AND RECOMMENDATION

6.1 Conclusion

A low speed wind tunnel study is carried on the UTM half model ranging from angle of attack of 0 deg to 24 deg at Reynolds number 0.5x10^6, 1.0x10^6 and 1.5x10^6. It is found that there is laminar bubble separation at 50% span when the flow in the test section is at Reynolds number 0.5 x 10^6 and once the Reynolds number is increased to 1.0 x 10^6 and 1.5 x 10^6, there is no sign of laminar separation bubble as the flow is in turbulent regime. It is found the lift coefficient at 50% span, flow fully separates at α = 8 deg for Re 0.5x10^6, α ≈ 9 deg for Re = 1.0x10^6 and α = 10 deg for Re = 1.5x10^6. Comparing to the lift coefficient obtained from the balance data, both results agreed that the flow separates from angle of attack of 8 deg to 10 deg for all Reynolds number. From this experiment, it can be concluded that as the Reynolds number increase the angle of attack for the flow to separates also increases. Finally, the flow visualization technique using threaded tuft shows that after angle of attack of 10 deg almost 70% of the wing span flow separates which causes the model to reach stall.

6.2 Recommendation

In the experimental study of flow separation on UTM half model which is a generic model of a transport aircraft using pressure coefficient method shows a reasonable result. Nevertheless, to have a better view of flow separation on a model methods like smoke test or PIV can show better result as the flow behavior can be clearer observed and the flow around the tapered-swept wing can be seen too. . Flow visualization such as applying fluorescent oil on the model should have been done so the flow field on the model could have been seen since this is another good way of studying flow separation. Measuring the pressure coefficient around the local chord at 50% span does not show the flow around the entire wing. In addition, the amount of pressure tap at 50% span should be increases so the pressure changes at each station can be measured precisely. Since, there was not enough pressure tap near the leading edge, the point of separation, transition and reattachment for laminar separation at Reynolds number at 0.5x10^6 could not be measured accurately.

ACKNOWLEDGMENTS

First and foremost, I would like express my sincerest gratitude to my UGP supervisor, Dr. Shabudin bin Mat for his guidance, advice, ideas throughout the completion of this UGP.

I would to take this opportunity to thank Mr. Sallehudin for his help and also ideas. Special gratitude goes to the staff of the mechanical faculty lab for their guidance and help.

I would also like to thank my family and friends for their moral support and ideas throughout the completion of this thesis.

REFERENCES

1. Durand, W. F., Melvill Jones, B. & Kerber, L. (1935). *Aerodynamic theory*. Berlin: Springer.
2. Munson, B. R., Young, D. F. & Okiishi, T. H. (2002). *Fundamentals of fluid mechanics*. New York: Wiley.
3. Clancy, L. J. (1975). *Aerodynamics*. New York: Wiley.
4. Flight Training Instruction Aerodynamic Workbook. (2009). Lexington: United States Navy.
5. Desktop.aero. (2013). *Applied aerodynamics, a digital textbook*. [online] Retrieved from: http://www.desktop.aero/appliedaero/preface/welcome .html [Accessed: 28 Dec 2013].
6. Russell, J. (1979). Length and bursting of separation bubbles: a physical interpretation.
7. Gencc, M., Karasu, . and Hakan Accikel, H. (2012). An experimental study on aerodynamics of NACA2415 aerofoil at low Re numbers. *Experimental Thermal and Fluid Science*, 39, pp.252--264

.

Journal of Aeronautical
-Science and Engineering-, Vol.1

February 28, 2015

Wing-In-Ground Craft for Marine Rescue Operation

Jaswar.Koto,[a,b] * and A.S.A.Kader,[c]

[a)]*Department of Aeronautic, Automotive and Ocean Engineering, Faculty of Mechanical Engineering, Universiti Teknologi Malaysia,*
[b)]*Ocean and Aerospace Research Institute, Indonesia*
[c)]*Marine Technology Center, Universiti Teknologi Malaysia, Johor, Malaysia*

*Corresponding author: jaswar.koto@gmail.com

Paper History

Received: 1-February-2015
Received in revised form: 20-February-2015
Accepted: 26-February-2015

ABSTRACT

This study aims to investigate the feasibility of wing in ground (WIG) craft used for marine rescue operation in Kepulauan Riau, Indonesia. Simulation code is developed using visual basic 2010 language. In the simulation, the rescue operation area was divided into two zones. Simulation result showed that the travelling time of WIG to reach the accidents location is less than 1.2 hour.

KEY WORDS: *Sea Accident; Marine Rescue Operation; Wing-In-Ground.*

NOMENCLATURE

WIG	Wing-In-Ground
IMO	International Maritime Organization
DOC	Direct Operating Cost
RCC	Rescue Coordinate Centre
SMC	Search and rescue Mission Coordinator
T_a	Time annual utilization

1.0 INTRODUCTION

Kepulauan Riau is a province one of the nation of Indonesia. Total area of Kepulauan Riau Province is 253,420 km^2 consist of 242,825 km^2 (96%) by sea, and the land area is 10,595.41 km^2 (4%). Marine transportation plays a very important to support the smooth flow of people, goods, and services.

Currently, search and rescue facilities in Kepulauan Riau Province there are only in Bintan. They have 1 unit rescue boat measuring 28.5 meters and has 10 units rubber boat.In the last two years (2010-2011) occurred 53 ship accidents in Kepulauan Riau province, with the number of victim 444 people, 381 people is survived, 37 people is died and 26 people is lost. Many people are dead and missing, caused due to lack facilities of rescue operations, the length of the evacuation process is done, and addition to the location of current rescue facilities were less strategic, considering the Riau archipelago 96% is the sea.

Therefore, it is necessary alternative equipment for rescue operations, to complement the limitations of the existing facilities. This paper propose wing in ground for alternative equipment in rescue operation. In addition, the position the central office of search and rescue is also a consideration. The position of the rescue facilities should have been more strategic to reach all areas of Kepulauan Riau Provinces with a faster time. So that, in case of any accident, the rescue transports can reach the target point and moves more flexibly to minimize casualties.

The paper discusses initial and optimal location for rescue facilities and time for rescue operation in Kepulauan Riau based on International Maritime Organization requirement. International Maritime Organization requirement, an emergency, passengers should be able to leave the ship with time 60 minutes. To find an initial and optimal position of rescue facilities in the Kepulauan Riau, researcher using the Great Circle Distance-Spherical Trigonometry Formula and statistical of Standard Error, in order that rescue facilities can be work an optimal. For calculating and mapping, researchers using visual basic programming, to make it more simple and automatic.

2.0 WING-IN-GROUND CRAFT

2.1. Types of Wing-In-Ground Craft

A wing-in-ground (WIG) craft is craft having capability to operate completely above the surface of the water which is created by aerodynamic lift due to the ground effect between the craft and the water's surface. WIG craft is capable of operating at speeds in excess of 100 knots and only apply to carry 12 passengers or more. The speed advantage of Wing in ground craft over conventional marine vessels and no special landing is required as helicopter and airplane, may well provide the reason for considering Wing in ground craft for particular applications.

The International Maritime Organization recognizes three classes of ground effect craft:

- Type A: a craft which is certified for operation only in ground effect;
- Type B: a craft which is certified to temporarily increase its altitude to a limited height outside the influence of ground effect but not exceeding 150 m above the surface; and
- Type C: a craft which is certified for operation outside ground effect and exceeding 150 m above the surface.

Configuration of wings for WIG can be classified into three as follows:

- Inverse Delta wing allows stable flight in ground effect through self stabilization. This wing is classified as Class B form of ground effect craft.
- Ekranoplan wing is significantly shorter than comparable aircraft, and this configuration requires a high aft-placed horizontal tail to maintain stability. The pitch and altitude stability comes from the lift slope difference between a front low wing in ground and an aft, higher-located second wing nearly out of ground effect.
- Tandem Wing can have two configurations: a biplane-style and a canard-style. A Tandem Wing Style with double-wing system is self-stabilizing and provides secure, comfortable and high-efficiency operation

2.2. WIG for Rescue

There are some theories clarify about Wing In ground can be used for search and rescue operation. Here is some of the theory which stated. According to Sungbu Suh, et al (2011), Du mian-yin and chen pei (2010),Han-Koo Jeong et.al (2010), Belavin, Volkov et al. and Hooker, in Kirill V. Rozhdestvensky (2006), Lee Qihui (2006), Graham K Taylor (2006), Quah Yong Seng, Jonathan (2005), Alexander Nebylov (2006), Graham Taylor (2003), Nikolai Kornev and Konstantin Matveev (2003), Seung-Hyun gwag (1997), E.A.Aframeev (1998), all of the they say wing in ground can be used for rescue operation.

According to Quah Yong Seng, Jonathan (2005), potential benefits of Wing In Ground is :Wing In Ground craft can fulfill the need for increased speed of marine transport and may thus fill the gap between shipping and aviation, WIG boats achieve high speeds while still maintaining high efficiency, especially when compared to other high speed marine craft, Due to the marine nature of Wing In Ground boats their operating cost are low as compared to aircraft, The infrastructural requirements for Wing In Ground boats are very low, any existing port is sufficient., Especially in a wavy sea the comfort level in cruise is very high as compared to other high speed marine craft.

According to Graham K Taylor (2003) & (2005), its main attributes wing in ground is :Turning the business machine faster, bringing destinations closer together, opening new routes within acceptable journey times, No sea motion, or sea sickness Low fatigue for occupants or equipment, No wash, no environmental damage to waterways, no effect on other waterway users, Immune to sea or river currents, will not hit floating objects such as driftwood, whales, etc, Shallow water operation, unaffected by tidal variation/water level, In the rescue environment Wing In Ground attributes are: Ability to cover a wide area within a short time, Rapid response capability – rapid closure.

Based on paper made by E. A. Aframeev, 1998, he said : Global sea rescue system is a worldwide concern to develop effective rescue measures on the high seas, the creation of global international sea rescue system based on the heavy WIG is the challenge for the international community. Experience shows that it is very difficult if not impossible to provide timely aid at wreckages and ecological disasters at sea. Use of seaplanes is often limited because of unfavorable meteorological conditions, whereas use of helicopters is restricted to coastal areas. Until now, the main means of rescue (salvage) on water has been ships finding themselves accidentally near the disaster area and hardly suitable for this purpose.

It should be emphasized that the effective rescue may be carried out if two components are available: quick notification about the catastrophe and quick arriving to the rescue means to the point of distress (E. A. Aframeev, 1998).

2.3. Mathematical Formulation

Initial and optimal location, distance and time are firstly are determined before cost estimation. In the present study, the initial location, distance and time are determined using real data of ship by accident in the form of latitude and longitude using the Great Circle Distance- Spherical Trigonometry Formula as follows:

$$D = R\ arccos[sin(lat_1)sinsin(lat_2) + cos(lat_1)cos(lat_2)cos(lon_2 - lon_1)] \quad (1)$$

where R is the radius of the earth in whatever units desire. The value is R=3437.74677 (in nautical miles), $R = 6378.7$ (in kilometers), $R = 3963.0$ (in miles).

At the calculate time used the Great Circle Distance Formula divided by speed of ship (V). The Algorithm of Spherical Trigonometry in determining the initial location (Jovin. J. Mwemezi. 2011).

i. Express latitudes and longitudes given in degree as radians :

$$R = \frac{deg}{180}\ \pi \quad (2)$$

ii. And then determine the initial coordinate of the new position (x^*, y^*), is defined by centre of gravity formula:

$$x^* = \frac{\sum w_i x_i}{\sum w_i} \quad (3)$$

$$y^* = \frac{\sum w_i y_i}{\sum w_i} \quad (4)$$

In order to get a range of optimal position, error of initial position is firstly calculated. In this case use a statistical of standard error. The standard error of a statistic is the standard deviation of the sampling distribution of that statistic (David Lane's, 2011). It is the standard deviation of the sampling distribution of the initial position. The formula for the standard error of the initial position is:

$$\sigma_M = \frac{\sigma}{\sqrt{n}} \quad (5)$$

Where σ is the standard deviation of the original distribution and n is the sample size (the number of scores each initial position is based upon).

To Estimate of Total Direct Operating Cost, Albeit various methods of cost analysis have been used to calculate operating costs, Chin Su Peak. (2006) (as cited in Akagi's, 1993) formula is suited to estimate direct operating costs ($per\ seat \cdot km$).

$$DOC = \left[\left\{\frac{1-r_v}{A} + r_{ins} + r_{int}\right\} + r_m\right]\left(\frac{K_s}{N_p V_s}\right)\frac{1}{T_a} + \left(\frac{C_{fu} M_f}{R N_p}\right) + \left(\frac{S_c N_c}{N_p V_s}\right) + \frac{1}{T_a} \quad (6)$$

where r_v is rate of residual value, A is amortization, r_{ins} is annual rate of insurance, r_{int} is annual, rate of interest, r_m is annual rate of maintenance, K_s is price of the vehicle, N_p is number of passenger, V_s is vehicle speed (km/h), T_a is time annual utilization (in hours), C_{fu} is price of fuel per kg, including lubricant, M_f is mass of the fuel, R is range (km), S_c is average yearly crew cost per person, N_c is number of crew.

The annual utilization time (T_a) has used the following formula taken by Akagi (1993).

$$T_a = n_a\left(\frac{t_d}{t_r + {}^{L_R}/_{V_s}}\right) \cdot \left(\frac{L_R}{V_s}\right) \quad (7)$$

where n_a is annual number of operating days, t_d is number of operating hours per day, t_r is terminal hours per service, L_R is length of the route.

3.0 METHODOLOGY

To conduct a systematically and thoroughly research, the research methodologies are based on the research process. The research process is a sequence of steps, which allow the researcher to create the structure and plan to investigate to problem selected for study. The general framework of proposed study is as shown in Figure 1. The following section will discuss the processes in detail.

In the literature review, researchers have searched many papers or journal which states that free wing in ground can be used for facilities of rescue operations. After learning that the wing in ground can be used as a facility of rescue operations, researchers must know the element - element that influence or are a barometer of the wing in ground more economical than the current of rescue operations. Based on survey data, current rescue cannot reach the whole sea area in the Kepulauan Riau province with a fast time. So, it requests to make feasibility study to find the strategic positioning as station of rescue facilities that means the rescue operation could be operating optimally.

In theoretical description is a little knowledge about the wing in ground, search and rescue operation, great circle distance-spherical trigonometry, statistical of standard error formula is needed to understand what they are actually.

The purpose is to review some references, to know the basic theory more specific. In data collecting, the data researcher collects is about current rescue boat specifications, the wing in ground specification, data by accident, and guidelines for evacuation analysis for new and existing passenger ships. For specifications of current rescue boat accident and data by accident, researcher get from the Search and Rescue Agency in Kepulauan Riau Province, while the data on the Wing in Ground (WIG) and Guidelines For evacuation analysis for new and existing passenger ships, researcher got from some journal / paper, and the internet. From the data collecting, researcher to identify research variables, in this thesis research variables are time, distance, speed, and coordinate.

Mathematical model, in this thesis about initial and optimal location, distance and time, and then estimates the cost. After mathematical modeling, mapping and simulation are created. The mapping and simulation were using visual basic 2010 software. Mapping done to visualize the distribution of accident, so it can determine its position with certainty, not just imagined. And then simulation is carried out simulation calculation of time, distance, and cost, to make it more automatic and simple.

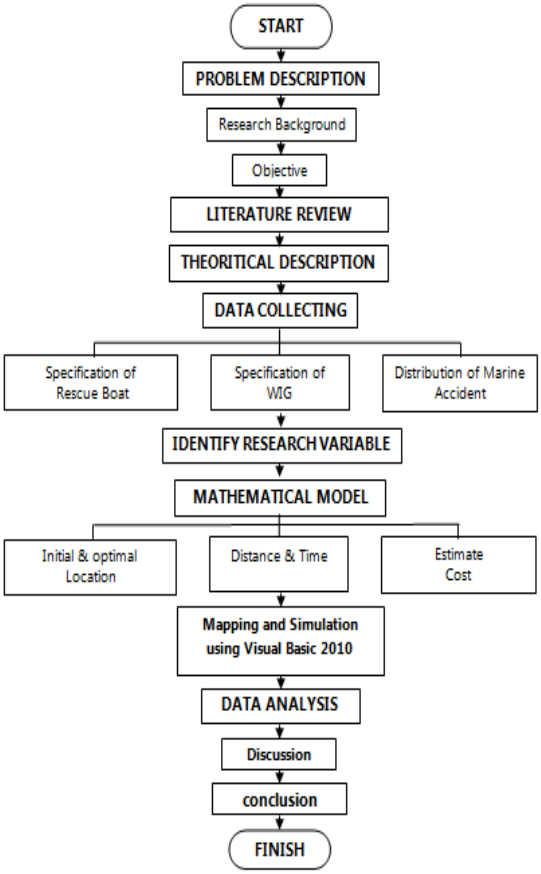

Figure.1: Flow Chart of Research Activity.

4.0 SIMULATION AND DISCUSSION

After napping in visual basic, it can be seen from the position of current facilities and distribution of accidents at sea that occurred in the Kepulauan Riau Province in 2010-2011 as shown in figure 2.

Using the current position rescue and distribution facilities accidents, the distance and time required to reach the crash site of each type of vehicle are determined. In this case, the current rescue facilities and wing in ground that has been selected.

The longest distance from the accident is 580.2 km and the shortest distance is 11.18 km. While the time required of current rescue to reach the accident site very long, there are up to 12.5 hours for the longest distance and up to 0.24 hours for the closest distance.

International Maritime Organization requirement, an emergency, passengers should be able to leave the ship with time 60 minutes. To fulfill International Maritime Organization requirement, this study propose wing in ground for rescue operation.

With the current position of rescue facilities, used wing in ground to rescue operation. When using the wing in ground facilities, is also too much time to cover the entire distribution of a ship accident of achieving 3.04 hours for the longest distance and 0.058 hours for the shortest distance.

Based on the distance between the position of the rescue facilities with distribution of ship accident happened in the Kepulauan Riau 2010-2011, some cost in rescue operation is calculated according to the data obtained from references and the data obtained from the calculation program, for current rescue facilities, Operation Costs During the Rescue Operation is Fixed Cost per Capacity-Speed = 0.2224, Annual Utilization = 70.1 and Fuel Cost = 25822, and while for wing in ground, Operation Costs During the Rescue Operation is Fixed Cost per Capacity-Speed = 0.0229, Annual Utilization = 14.2 and Fuel Cost = 6352.2.

It can be concluded that using a single rescue facilities are not optimal, given the area of Kepulauan Riau 96% is sea. Moreover, it cannot perform a rescue operation with quickly based on international maritime organization requirement. In view of this fact, researchers proposed must have a minimum two position of rescue facilities in Kepulauan Riau. In this case, the researchers divided the Kepulauan Riau into two region.

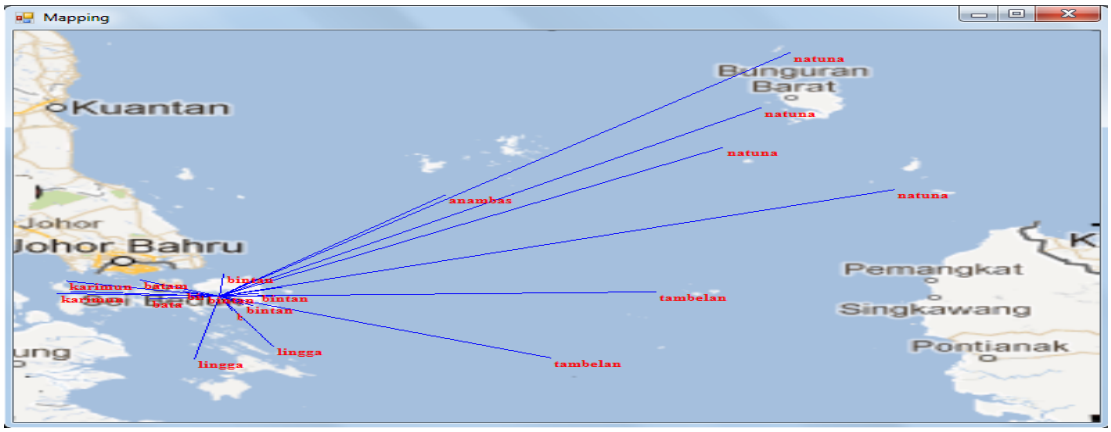

Figure.2 Current position of Rescue Facilities and Distribution of Accidents

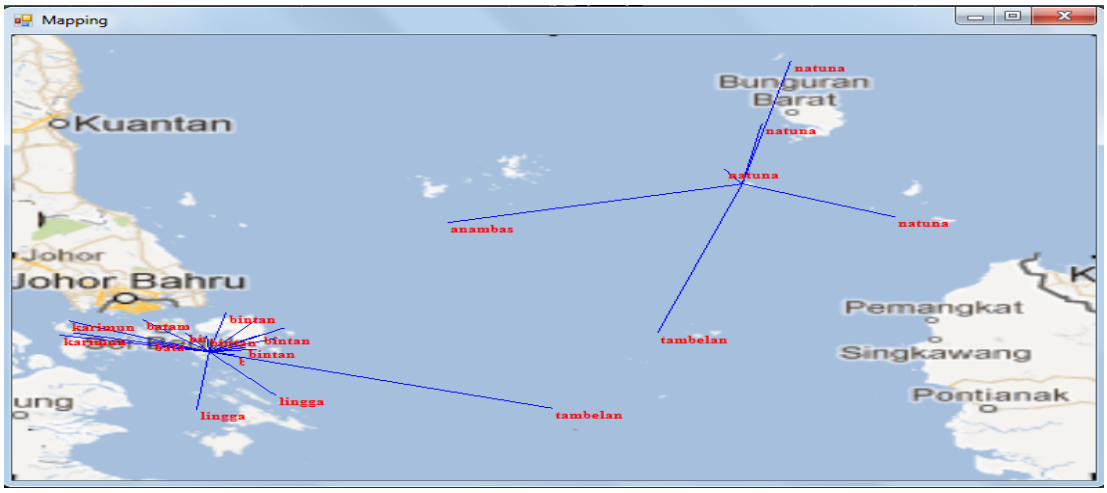

Figure.3 Optimal Position of rescue facilities Region 1 and Region 2.

From an optimal range of position is obtained, we can determine the optimal position of rescue facilities in the nearby island of optimal range position.

Researchers determined the optimal position of region 1 is the longitude 104.36256 and latitude 0.74568, while in region 2 is on the longitude 107.79373 and latitude 3.00338, as shown in figure 3.

The time it takes current rescue facility in region 1 to reach the accident site in the region is still also need much time, up to 5.59 hours for the longest distance and 0.41 hours for the closest distance. While in region 2, the current rescue takes 4.99 hours for the longest distance and 0.562 hours for the shortest distance.

Region 1 it takes wing in ground, only 1.35 hours for the longest distance and 0.1 hours for the shortest distance. While in region 2, which is only 1.2 hours for the longest distance and 0.13 hours for the shortest distance.

Based on the distance between the position of the rescue facilities with distribution of ship accident happened in the Kepulauan Riau 2010-2011, some cost in rescue operation is calculated according to the data obtained from references and the data obtained from the calculation program, for current rescue facilities region 1, Operation Costs During the Rescue Operation is Fixed Cost per Capacity-Speed = 0.2224, Annual Utilization = 19.3 and Fuel Cost = 8686.1, and while for wing in ground, Operation Costs During the Rescue Operation is Fixed Cost per Capacity-Speed = 0.0229, Annual Utilization = 3.2 and Fuel Cost = 2136.8. Then for current rescue facilities region 2, Operation Costs During the Rescue Operation is Fixed Cost per Capacity-Speed = 0.2224, Annual Utilization = 15.6 and Fuel Cost = 5998.7, and while for wing in ground, Operation Costs During the Rescue Operation, Fixed Cost per Capacity-Speed = 0.0229, Annual Utilization = 2.9 and Fuel Cost = 1475.7.

5.0 CONCLUSION

Based on current position of rescue facility, it is required a lot of time to reach the accident location in order to perform rescue operation, reaching up to 12.5 hours. When using the wing in ground facilities, it also needs time to cover the entire distribution of a ship accident of achieving 3.04 hours. The optimal for rescue facilities of region 1, at the latitude 0.74568 and longitude 104.36256, current rescue facility required up to 5.6 hours to reach the accident area, while the wing in ground facilities required up to 1.3 hours. The optimal for rescue facilities of region 2, at the latitude 3.00338 and longitude 107.79373, current rescue facility required up to 5 hours to reach the accident area, while the wing in ground facilities required shorter time that is up to 1.2 hour. So, wing in ground can be improved rescue operations in the Kepulauan Riau, given the current rescue cannot cover all the whole area quickly based on international maritime organization requirement, although two rescue boats used in the two regions. In addition, the cost incurred rescue boat more expensive than the wing in ground, during the rescue operation.

ACKNOWLEDGEMENTS

The authors would like to convey a great appreciation to Departement Perhubungan Kepulauan Riau, Indonesia and Universiti Teknologi Malaysia, Malaysia for supporting this research.

REFERENCE

1. Alexander Nebylov. 2006. *Wing-In-Ground Vehicles: Modern Concepts Of Design, Automatic Control, Applications*. State University of Aerospace Instrumentation, Saint-Petersburg, Russia
2. Akagi, S. (1993). A Study of Transport Economy and

Market Research for High Speed Marine Passenger Vehicles. *Proceedings of Fast 93, Second International Conference on Fast Sea Transportation. (pp.1129-1142).* Yokohama: Society of Naval Architects of Japan.

3. Chin Su Peak. 2006. *The Viability Of Commercializing Wing-In-Ground (Wig) Craft In Connection With Technical, Economic And Safety Aspects Followed By Imo Legislation.* World Maritime University
4. David Lane's. 2011. *HyperStat Online Statistics Textbook*. Departments of Psychology, Statistics, and Management. Rice University.
5. Du mian-yi, chen pei. 2010. Dynamic aerodynamic characteristics simulation of WIG effect craft based on moving overset grid. *Proceedings of the 13th asian congress of fluid mechanics*, Dhaka, Bangladesh.
6. E.A.Aframeev . 1998. *Conceptual bases of WIG craft building: ideas, reality and outlooks*. Krylov Shipbuilding Research Institute 44, Moskovskoe Shosse Saint Petersburg, 196158 Russia
7. Graham.K.Taylor. 2006. Innovation Dying Of Apathy: Wig – A Case Study. *RINA International Conference.*
8. Graham Taylor.2003.Re-Defining Sea Level: The Hoverwing Wing In Ground Effect Vehicle. *Air Cushion Technology Conference & Exhibition*, England
9. Han-Koo Jeong et.al. 2010. *On the structural test of 1.5-ton test WIG craft*. Department of Naval Architecture, Kunsan National University, Gunsan, Jeonbuk 573-701, Korea.
10. *International Maritime Organization*, Retrieved: 30 December 2011
11. Jovin J. Mwemezi and Youfang Huang. 2011. *Optimal Facility Location on Spherical Surfaces: Algorithm and Application*. Logistics Research Center, Shanghai Maritime University
12. Kirill V. Rozhdestvensky. 2006. *Wing-In-Ground Effect Vehicles*. Saint-Petersburg State Marine Technical University, Lotsmanskaya 3, Saint-Petersburg, 190008, Russia
13. Sungbu Suh, et al.2011. Numerical And Experimental Studies On Wing In Ground Effect. *International Journal of Ocean System Engineering.*
14. Lee Qihui.2006. *Stability, Control and Performance for an Inverted Delta Wing-In-Ground Effect Aircraft*. Department of Mechanical Engineering. National University of Singapore.
15. Quah Yong Seng, Jonathan.2005. *Stability, Performance & Control for a Wing in Ground Vehicle*. Department of Mechanical Engineering. National University of Singapore.
16. Seung-Hyun gwag. 1997. Numerical Study on 3-Dimensional Power-Augmented Ram Wing in Ground Effect. *Proceedings of the Seventh (1997) International Offshore and Polar Engineering Conference Honolulu*, USA.

Published

ISOMAse
Resty Menara Hotel
Jalan Sisingamangaraja No.89
Pekanbaru-Riau, INDONESIA
http://www.isomase.org/

Edited

Building P-23, Room: 314
Department of Aeronautics,
Automotive & Ocean Engineering,
Faculty of Mechanical, Universiti
Teknologi Malaysia, MALAYSIA
http://web1.fkm.utm.my/

ISSN: 2442-6407

Printed

Teknik Mesin
Fakultas Teknik,
Universitas Riau, INDONESIA
http://www.unri.ac.id/en

Organized

Ocean & Aerospace Research
Institute, Indonesia
Pekanbaru-Riau, INDONESIA
http://isomase.org/OCARI.php/

Supported

Mechanical Chapter of the
Institution of Engineers,
INDONESIA

Malaysian Joint Branch Royal
Institution of Naval Architects &
Institute of Marine Engineering,
Science and Technology
-Southern Chapter (MJB RINA
&IMarEST – SC)-